Available online at www.sciencedirect.com
SCIENCE DIRECT
Polymer 46 (2005) 4013–4022
polymer
www.elsevier.com/locate/polymer

Ionomer–silica hybrids via sol–gel reaction

Yan Gao[a], Namita Roy Choudhury[a,*], Naba Dutta[a], Luc Delmotte[b]

[a]*Ian Wark Research Institute, ARC Special Research Centre, University of South Australia, Mawson Lakes, South Australia*
[b]*Ecole National Superior De Chimie De Mulhouse, Mulhouse, France*

Received 18 August 2004; received in revised form 21 January 2005; accepted 16 March 2005
Available online 22 April 2005

Abstract

Ionomer–silica hybrid materials were made from polyethylene-*co*-acrylic acid neutralized by a zinc salt (PI) and tetraethoxy silane (TEOS) via the sol–gel reaction. The effects of various experimental parameters such as solvents, H_2O/Si ratio and the amount of TEOS in the ionomer solution on the hybrid structure and properties were examined. The spectroscopic results show that solvents do not affect the structure of the hybrids, but influence the thermal properties. The hybrids made using highly polar solvent exhibit better thermal stability and dynamic mechanical properties at high TEOS contents. The amount of water used for hydrolysis and subsequent condensation play a significant role in the network formation. The varying amount of TEOS in solutions gives rise to different silica content of the hybrid. Above 50 wt%, the sample becomes opaque due to silica aggregation. The high ratio of H_2O/Si leads to phase separation during the reaction. Transparent hybrid materials can only be obtained when the ratio of H_2O/Si is below 5.

Keywords: Ionomer; Sol–gel reaction; Solvents

1. Introduction

A rapidly growing area of nano-engineered materials is polymer–inorganic hybrids, due to their promise to provide lighter weight alternatives to conventional-filled plastics with additional functionality associated with nanoscale-specific value-added properties [1–4]. Hybridisation generally leads to very fine dispersion of the inorganic phase into the polymer matrix with significant enhancement in properties such as thermal stability, mechanical properties, gas permeation, solvent resistance, optical and electronic properties, etc. The properties of nano-composite materials depend not only on the properties of the individual component but also on their morphology and interfacial characteristics. There are several routes to prepare organic–inorganic hybrids such as intercalation, electrocrystallization, sol–gel processes, etc. The sol–gel process with its unique mild processing characteristics and ease of control is the most common method for preparing pure and well-controlled composites [5–9]. This process includes two reactions: the hydrolysis of a metal alkoxide, and subsequent condensation producing alcohol, water and a metal oxide network. The most widely used metal alkoxide is silicon alkoxide, such as tetraethoxy silane (TEOS) or tetramethoxy silane (TMOS).

Depending on the strength or level of interaction two kinds of links between organic and inorganic phases are observed [10,11]: (i) physical or weak phase interactions, e.g. hydrogen bonding, van der Waals interaction achieved through simple physical mixing; (ii) strong chemical bonds either covalent or ionic–covalent bonds. Various hybrids, which have been reported to date, are mostly hydrogen bonded and in some cases covalently bonded. Greso et al. [12] used Nafion with TEOS to make hybrids with chemical bonds between organic and inorganic compounds. Wojcik et al. [13] reported a hybrid made by a ring-open reaction of 2-methyl-2-oxazoline to form silane-coupling agents on the nanoscale. Yang et al. [14] prepared PMMA–silica (PMMA: polymethyl methacrylate) hybrids, which were formed by covalent bonding between inorganic components and the polymer. Landry et al. [15] reported the PMMA–silica hybrids prepared via the sol–gel reactions, where hydrogen bonding was prevalent. Schiavon et al. [2] reported different structures for PMMA–silica hybrids produced using different catalysts. Acid catalysts can

* Corresponding author. Tel.: +61 8 8302 3719; fax: +61 8 8302 3755.
E-mail address: namita.choudhury@unisa.edu.au (N.R. Choudhury).

0032-3861/$ - see front matter © 2005 Elsevier Ltd. All rights reserved.
doi:10.1016/j.polymer.2005.03.053

cause significant phase separation. However, Landry et al. [15] demonstrated that nanoscale silica domains appeared in acid environments and extensive phase separation occurred in basic environments. These observations clearly indicate that the structure of hybrids strongly depends on the reaction conditions. Theoretically, the mole ratio of H_2O/Si in the reaction mixture is 4 for complete hydrolysis. If the amount of water increases, complete hydrolysis of silicon alkoxide takes place before significant condensation occurs and the completion of reaction is delayed.

The rates of the hydrolysis and condensation reactions are affected by the solvent polarity. Jonas [16] and, Orcel and Hench [17] found that partly substituting methanol with formamide slows down the hydrolysis reaction, but speeds up the condensation reaction under neutral conditions. This is because formamide, with high dielectric constant can form stronger hydrogen bonds than methanol, and its viscosity is much higher. The concentration of silicon alkoxide is another parameter that affects the structure and properties of the hybrids. A high silicon alkoxide concentration can cause brittleness in the hybrid material because it leads to the formation of large amounts of silica. Zoppi et al. [18] prepared Nafion–silica hybrid materials using up to 80 wt% TEOS. In order to increase the flexibility of the samples, TEOS was substituted partially by TMDES (1,1,3,3-tetramethyl-1,3-diethoxy disiloxane).

Ionomers have unique properties due to their unique architecture. In PI, there is less than 15 mol% of ionic groups, which aggregate to form clusters. In solution they can have different structures due to the polymer (hydrophobic) and ionic (hydrophilic) parts. Kim et al. [19] studied the network structure of tailor-made urethane acrylate ionomers in different solvents and three types of structures were proposed. While polymer phase separation can be observed at low polarity solvents (toluene) as dissolution of polymer chains only leads to ionic group aggregation. However, DMSO (dimethyl sulfoxide) dissolves both the polymer and ionic parts to form a homogeneous network structure. Polar solvents increase the interaction between the polymer chains, and destroy the strong ionic association of the cluster structure. As the interaction between ionic groups varies in different solvents, this may affect the morphology of the silica network formed via the sol–gel reaction. To date only a few ionomer–inorganic hybrid materials have been reported using Surlyn [20,21], Nafion [12,22] and PI [23,24] ionomers. However, study of the effects of various sol–gel process parameters on the structures and properties of hybrid materials is scanty.

In this paper, we report on the properties of PI–silica hybrids prepared with various amounts of TEOS in ionomer, various H_2O/Si ratios and different solvents. The hybrid materials were characterized using photo-acoustic Fourier transform infrared spectroscopy (PA-FTIR), ^{29}Si solid-state nuclear magnetic resonance spectroscopy (^{29}Si solid-state NMR), transmission electron microscopy (TEM), thermogravimetric analysis (TGA), modulated differential scanning calorimetry (MDSC), dynamic mechanical analysis (DMA), small-angle X-ray scattering (SAXS), and wide-angle X-ray study (WAXS).

2. Experimental and characterization

2.1. Materials

PI ionomer (Iotek 4200-zinc salt of ethylene acrylic acid copolymer, melt index 3) was obtained from Kemcor Australia. It contained 11 wt% acrylic acid, of which 14 mol% is neutralized as a zinc salt. Tetraethyl orthosilicate (TEOS, 99% purity) was purchased from Aldrich. Butylamine (Aldrich) was used as a catalyst. Different solvents used were toluene, butanol, ethanol and propanol.

2.2. Preparation of the hybrids

The preparation of the hybrid has been reported in an earlier publication [23]. In general, PI was dissolved in the binary solvent mixture (toluene and an alcohol: 3:1) to form 10 wt% solution. In this work ethanol, propanol and butanol were used as co-solvents to toluene. TEOS, distilled water and butylamine mixture was then added into the solution. The content of TEOS in the mixture was 50 wt%. The ratio of TEOS/H_2O used was 1:4. The quantity of butylamine was 0.02 g. The reaction was continued for one hour at 80 °C with vigorous stirring. Finally, the mixture was poured into a teflon petri dish followed by heating in an oven at 80 °C, and ageing for one week. The amount of TEOS/Zn–PI was used in various weight ratios. Table 1 lists the amount of each component and solvents used.

In order to understand the effects of TEOS concentration on the sol–gel reaction, hybrids were prepared by changing the amount of TEOS. The solvent mixture was butanol and toluene. The composition of the ionomer (weight ratio) in the solution is listed in Table 2. PI–silica hybrids were prepared by changing the molar ratio of H_2O/Si from 1, 2, 5, 10, 25, 50 and 100. All the samples were prepared under similar processing conditions such as temperature and time, then tested 24 h after heat aging.

2.3. Sample characterization

2.3.1. Chemical structure

Photoacoustic Fourier transform infrared spectroscopy (PA-FTIR) was performed using a Nicolet Magna spectrometer (Model 750) equipped with a MTEC (Model 300) photoacoustic cell. The experimental conditions used were 8 cm^{-1} resolution, 256 scans and mirror velocity of 0.158 cm/s. The purge gas was helium at a flow rate of 10 cm^3/s.

The ^{29}Si solid-state NMR of the sample was performed using a Bruker MSL 300 spectrometer. The spectra of the samples were obtained using cross polarization and magic-

Table 1
Residue from TGA and crystallinity from XRD/ MDSC of various hybrids and ionomer

Sample	Solvents	TEOS wt%	Dielectric constant ε	TGA		Crystallinity wt%	
				Decom. temp. °C	Residue wt%	MDSC	XRD
PI	–	–	–	460.0	0	20.92	21.0
IE1	90Toluene/ 10ethanol	50	4.597	466.9	16	18.79	19.6
IE2	90Toluene/ 10ethanol	25	4.597	463.0	11	21.79	22.8
IP1	90Toluene/ 10propanol	50	4.187	467.1	13	19.78	22.9
IP2	90Toluene/ 10propanol	25	4.187	467.1	10	21.08	26.0
IB1	75Toluene/ 25butanol	50	6.160	468.5	19	15.39	15.5
IB2	75Toluene/ 25butanol	25	6.160	465.9	11	20.47	21.9

angle spinning (CP/MAS). The spinning rate used was 4 kHz. A radio frequency of 62.5 kHz was used for cross polarization and proton decoupling (90° pulse width for $^{1}H = 4$ μs). Standard Bruker 4 mm CPMAS probe was used.

Small-angle X-ray scattering (SAXS) experiments were performed at room temperature using compression-moulded films in a Bruker SAXS instrument. The sample-to-detector distance used was 62.7 cm. The X-ray source was from Cu K_α radiation of wavelength 1.54 Å. The scan of 2θ was from 0.15 to 5°. Wide-angle X-ray diffraction (WAXS) was performed at room temperature on compression-molded films using a Bruker 5005 X-ray diffractometer for the reflected diffraction mode. The Bruker X-ray instrument consists of a rotating anode source, pinhole collimation, and a two dimensional Hi-STAR detector for the transmission mode experiment. The scan was in the range of 5–30° at 1.0°/min.

2.4. Thermal analysis

Thermogravimetric analysis (TGA) was carried using a TGA 2950 thermal analyzer (TA Instruments). The sample was heated from room temperature to 600 °C at 10 °C min^{-1} under a nitrogen atmosphere at 50 ml/min. Differential scanning calorimetry (DSC) and modulated DSC of the samples were conducted using TA 2920 DSC in conventional and MDSC modes (TA Instruments) respectively. In the conventional DSC mode, the sample was heated from 30 to 120 °C at 20 °C/min, then cooled to 30 °C at 0.5, 2 and 5 °C/min cooling rate, finally heated to 120 °C at 2 °C/min in MDSC mode with an amplitude of modulation ±0.2 °C and a period of 40 s. The melting was recorded from MDSC run. The crystallization behavior of PI has been explained elsewhere [23].

Table 2
The effect of TEOS content on the nature of the hybrids

Sample	TEOS/ionomer weight ratio	Nature of the sample
1	10/90	Transparent
2	20/80	Transparent
3	30/70	Transparent
4	40/60	Transparent
5	50/50	Transparent
6	60/40	Not transparent, brittle
7	70/30	Not transparent, brittle
8	80/20	Not transparent, brittle

Dynamic mechanical analysis (DMA) was performed using DMA 2980 (TA Instruments). The module DMA multifrequency–multitension mode was used. All the samples were molded into a sheet, of 0.5 mm thick. The sheets were then cut into the size of 15 mm × 2 mm (length × width). The sample was heated from −150 to 100 °C at a heating rate of 3 °C/min. A frequency of 1 Hz and a static force of 1 N were used for all the experiments.

2.4.1. Microscopic investigation

Transmission electron microscopy (TEM) was used to study the morphology of the hybrid. The specimen was carbon coated before the test. The polymer samples were cut into long, narrow strips (approx. 50 nm × 0.2 mm) by ultramicrotomy using a diamond knife. The hybrid was deposited on a carbon-coated nitro-cellulose film supported by a copper mesh. The examination was carried out using a Philips CM200 transmission electron microscope operating at an acceleration voltage of 200 kV at different magnifications.

3. Results and discussion

3.1. Effect of solvents

The polarity of the mixed solvents can drastically affect the network structure of the hybrids due to different rate of

hydrolysis and the chemical equilibrium of the system. Table 1 lists the solvents used in this work and their respective dielectric constants. The dielectric constant of the mixed solvent is calculated (assuming that there is no solvent–solvent interaction) using the following equation: $\varepsilon_{mix} = W_1\varepsilon_1 + W_2\varepsilon_2$, where ε_{mix}, ε_1 and ε_2 are the dielectric constants of the mixed solvent, solvent 1 and solvent 2, W_1 and W_2 are the weight fractions of the solvent 1 and solvent 2, respectively. A mixture of toluene and butanol shows the highest value of dielectric constant amongst all the solvents.

3.2. Spectroscopic study

PA-FTIR spectroscopy was used to obtain information on the structure and chemical composition of the hybrids. If the condensation reaction is complete, silica is formed from TEOS via the sol–gel reaction. The characteristic peaks of silica can be observed from the PA-FTIR spectrum. Fig. 1 shows the spectra of the ionomer (PI) and the hybrids obtained using the different solvents (IE1, IP1 and IB1). It is obvious that the peaks from 1000 to 1200 cm^{-1}, 473 cm^{-1} appear in all the hybrid samples, but not in PI. This indicates that silica is formed via the sol–gel reaction in the hybrids. The peak at 1000–1200 cm^{-1} is due to asymmetric stretching vibration of the Si–O–Si bonds of the silica component, and the shoulder on the left side is due to different substructures between Si–O–Si groups, e.g. linear and cyclic (1063 and 1108 cm^{-1}). The shapes of the shoulders appear to be different in each sample. The content of the linear substructure is higher in IP1 than in other samples, which demonstrates that the substructure of silica can also be influenced by solvents. A low dielectric constant solvent develops relatively higher linear structure of silica, as dipolar attractions between chain segments exist in less-polar solvent. The band at 473 cm^{-1} is ascribed to Si–O–Si and/or SiOH groups, which does not show any difference in various samples. The presence of the band at 955 cm^{-1} reveals the existence of the SiOH group in each of the hybrid samples. This also indicates that an incomplete condensation reaction occurs in all samples using various solvent mixtures. The peak in the range of 3000–3680 cm^{-1} is ascribed to –OH group from alcohol, some residual water and solvent. The intensity of the peak can be affected by the nature and amount of alcohol, and the degree of incomplete condensation reaction. The bands at 2800–3000 cm^{-1} ascribed to C–H stretching of $–CH_2–$ and $–CH_3$ groups, which do not shift or change. The band for residual water appears at 1620 cm^{-1}. In addition, the C=O stretching vibration from the –COOH group at 1700 cm^{-1} does not shift in any sample indicating that no hydrogen bonds form between –COOH groups in PI and SiOR/SiOH.

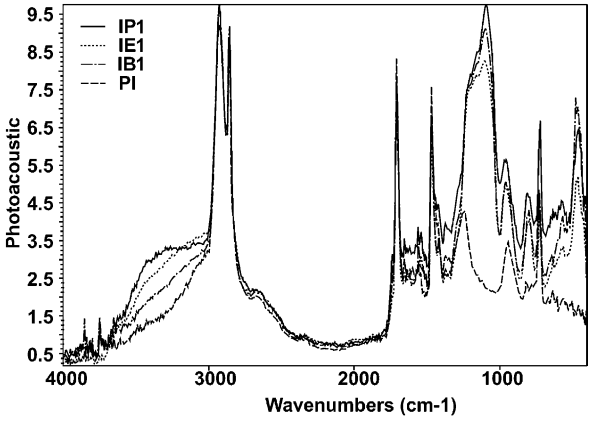

Fig. 1. FTIR spectra of PI, IE1, IP1 and IB1, showing the effect of various solvents on sol–gel reaction of ionomer.

The formation of the hybrids using various solvents occurs by the formation of silica from TEOS via the sol–gel reaction and the nature of the silicate structure in each sample can be clearly identified using ^{29}Si solid-state NMR. Although Si–O–Si groups are formed via the sol–gel reaction in every solvent, yet the condensation reaction may remain incomplete in each sample. ^{29}Si solid-state nuclear magnetic resonance spectroscopy (^{29}Si solid-state NMR) can be utilized to further demonstrate the structure of silica and the degree of silicon condensation. Fig. 2 shows the ^{29}Si solid-state NMR spectra of IP1 and IE1. The IB1 data was reported in an earlier paper [23]. It is clear that two kinds of silicon environments appear adjacent to each other in the range of -90 to -115 ppm in each sample due to Q_3 and Q_4, respectively. The Q_3 peak is larger in IP1 than IE1, while the Q_4 peak is smaller. The area ratio of Q_4/Q_3 is greater in IE1 than IP1. The degree of condensation can be evaluated from percent Q_4. It is clear from the spectra that the degree of silicon condensation using ethanol is higher than in propanol. Comparing the spectra of IP1, IE1 and IB1 [23], the peak area of Q_4 is in the order: IB1 > IE1 > IP1. This implies that the condensation reaction is affected by the polarity of solvents. Polar solvents can speed up the condensation reaction. Similar trends were observed by Jonas [16] and Orcel and Hench [17].

3.3. Compositional analysis and the thermal stability of the hybrids

TGA was used to investigate the thermal stability, the silica content and the onset of decomposition behavior of investigated samples. Fig. 3 shows the thermograms of PI, IE1, IP1 and IB1. Table 1 lists the silica content and the maximum decomposition temperature of each sample. The figure shows that the weight loss curves of the hybrids shift to higher temperatures in comparison to the neat sample, indicating higher thermal stability of the hybrids after the sol–gel reaction. The decomposition of the polymer in the hybrids occurs over a range of ~160 °C (350–510 °C). However, the decomposition temperature does not follow any particular order. There are marginal difference in thermal stability among the samples, and follows the order: IB1 > IP1 ≈ IE1, even though the silica content does not follow this trend. The silica content in the hybrid increases

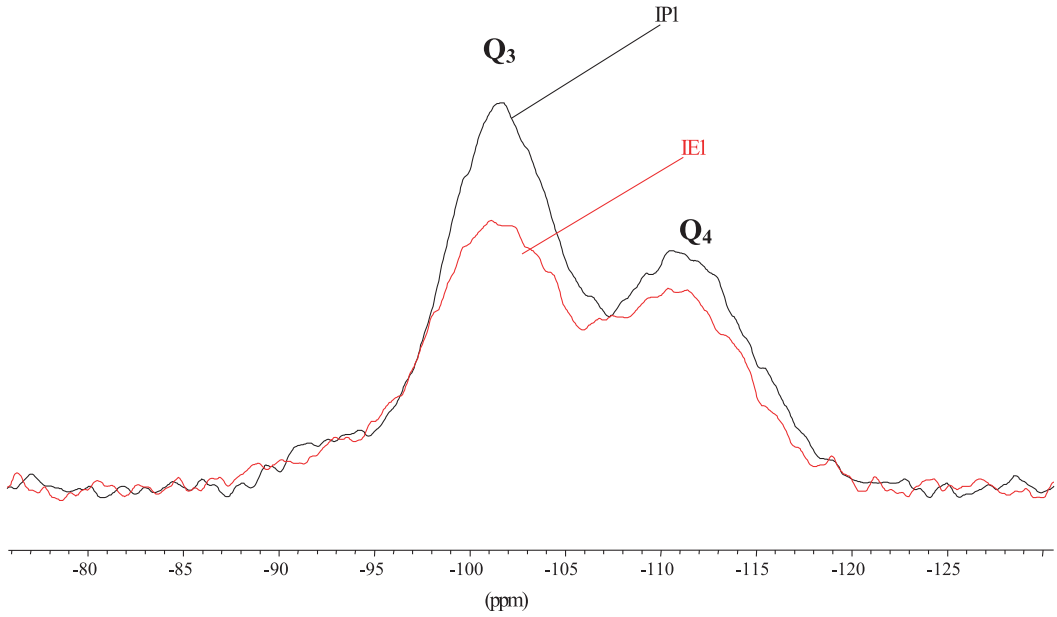

Fig. 2. ^{29}Si solid-state NMR spectra of IP1 and IE1.

with increasing polarity of the solvent at high TEOS proportion. The dielectric constant of the solvents follows the order: IB1 > IE1 > IP1. IB1 with highest thermal stability has the highest silica and the silica content of IP1 is lower than IE1. High dielectric constant and hydrophobicity of the solvent tend to disrupt not only the ionic bonds in solution [19] but also any hydrogen bonding present in the system. This can also influence the availability of water for the hydrolysis reaction. However, the silica content is more or less similar using different solvents when the TEOS proportion is 25%, although the thermal stability of IP2 is higher than IE2 and IB2. At low TEOS proportion, the solvents do not significantly alter the degree of reaction, but affect the thermal stability of the samples. The onset temperatures of chemical decomposition for all the hybrids do not vary, but remain lower than that of the ionomer. This is due to the presence of low molecular weight byproduct, such as water and alcohol, the solvents and further possible condensation of SiOH to silica [25].

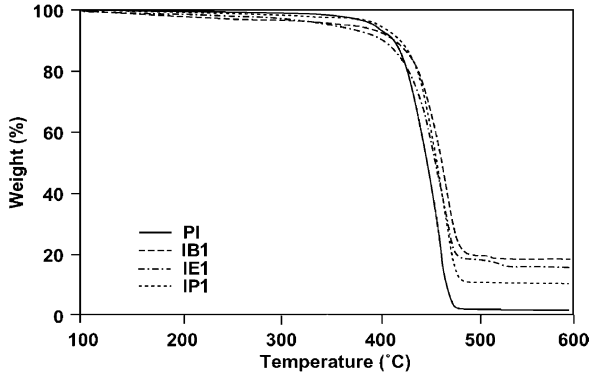

Fig. 3. Thermograms of PI, IE1, IP1 and IB1.

3.4. Morphological investigation

DSC was used to study the glass/cluster transition and the crystallinity of the materials. As the ionomer has both the cluster part and the hydrophobic ethylene part, two transition peaks are expected. Fig. 4 shows the DSC traces of PI, IE1, IP1 and IB1. The transition behavior of PI and the hybrids was reported earlier [23,26]. The peak observed at about 96 °C is the melting of polyethylene (PE) crystals, while the cluster transition occurs at about 50 °C. The peak at 50 °C for each of the hybrid samples becomes broader and smaller compared to the ionomer, and shifts. This indicates that the cluster morphology and transition change after the sol–gel reaction due to insertion of silica into the cluster. The PE melting peaks of the hybrids IE1 and IB1 do not change significantly. This also confirms the FTIR results that TEOS does not affect the polyethylene part of polymer chains. The peak of IP1 at 96 °C shifts to a slightly higher temperature due to reorganization of the polymer chains.

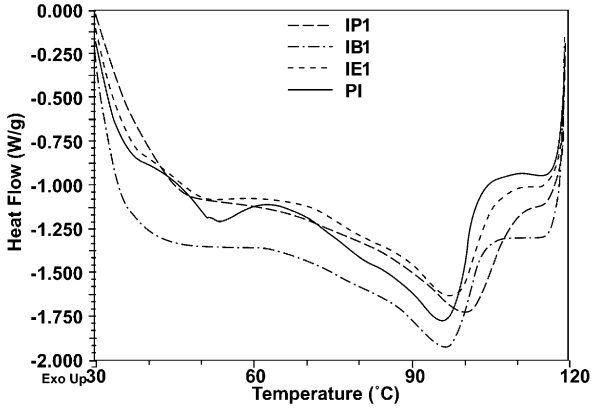

Fig. 4. Effect of solvent on the thermal transition behavior of ionomer.

The second heating cycle for IP1 shows the same melting temperature as the other samples. The total heat flow of the PE component of the hybrids in most cases is smaller than PI, indicating a reduction in the crystallinity of PI (Table 1).

MDSC was used to understand the effect of SiO_2 on the crystallinity of the ionomer in the hybrid. The total heat flow, reversing and nonreversing components of the heat flow were examined to study such behavior. Fig. 5 overlays the MDSC results of IE1 and IP1 at 2 °C/min cooling rate. The melting of polyethylene for all the samples occurs in the reversing and nonreversing heat flows. A shoulder appears on the left-hand side of the main melting peak in the nonreversing and total heat flows. This is due to folded chains and different morphologies [27]. However, the reversing heat flow signal of IP1 shows different behaviors with an exothermic, and an endothermic peak, while the reversing peaks of other hybrids are endothermic in nature. This indicates that not only crystallization but also some structural reorganization occurs. Table 3 lists the MDSC results for the ionomer and the hybrids. The total heat flow of each sample does not change with the cooling rate, however, the contributions of the reversing and nonreversing heat flow change. This is because the reversing and nonreversing signals can be affected by various experimental parameters, e.g. modulation amplitude, period, underlying heating rate and sample thickness. It is obvious that the growth of silica via the sol–gel reaction increases the reversing component, but reduces the nonreversing component and the total heat flow. The presence of silica enhances the melt entanglement density of linear polymers. The crystallinity of IE1, IP1 and IB1 is either similar or lower than PI, and it follows the order: IB1 < IE1 < IP1 (Table 1). At low TEOS concentration (25%), the hybrids (IP2, IE2 and IB2) show similar thermal behaviors in the reversing and nonreversing components as at 50% TEOS (Table 3). The silica contents in IP2, IE2 and IB2 are almost same, and so is the crystallinity of the polyethylene component of the hybrids.

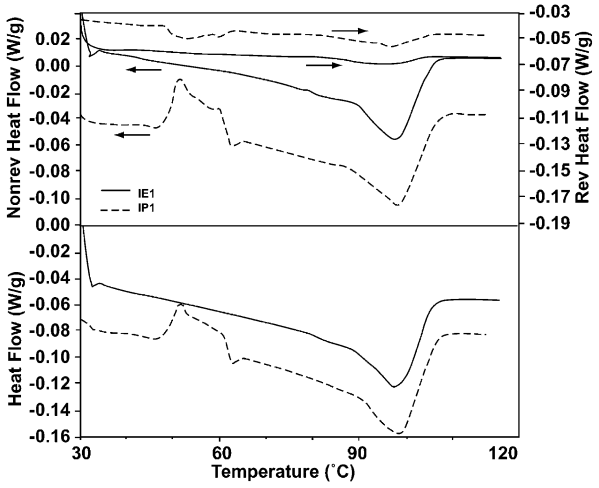

Fig. 5. MDSC curves of IE1 and IP1 at 2 °C cooling rate.

Table 3
MDSC results of PI and the hybrids

Sample	Cooling rate °C/min	Revers. HF J/g	Nonrevers. HF J/g	Total HF J/g
PI	0.5	12.0	52.6	64.6
	2	15.2	45.4	60.6
	5	20.4	40.3	60.8
IE1	0.5	13.2	44.5	57.8
	2	5.8	48.6	54.4
	5	11.8	38.7	50.2
IE2	0.5	13.9	48.2	62.1
	2	14.9	48.2	63.1
	5	20.2	41.6	61.6
IP1	0.5	4.5	52.8	57.3
	2	−0.1	55.5	55.2
	5	7.2	55.4	64.2
IP2	0.5	−2.0	66.5	63.6
	2	1.0	61.0	61.1
	5	0.0	58.0	60.7
IB1	0.5	16.7	34.6	51.4
	2	18.3	26.2	44.6
	5	22.5	25.6	48.2
IB2	0.5	9.8	53.9	63.8
	2	9.5	49.8	59.3
	5	15.1	44.5	59.7

WAXS measurement was used to obtain the microstructure and morphology of the hybrid polymers. Fig. 6 superimposes the WAXS curves of PI, IE1, IP1 and IB1. A sharp peak appears at around $2\theta \approx 20°$ in each case. The sharp peak relates to the crystalline component of polyethylene. The shoulders are associated with the amorphous component of polyethylene. The sharp peaks of IE1 and IB1 do not shift compared to PI, which indicates that d spacing of polyethylene does not change. Thus, the presence of silica does not alter the morphology of PE crystal. This result is in line with FTIR and MDSC results. Table 1 lists the crystallinity of each sample from WAXS results using peak fitting programs. The results are in line with the MDSC results. The peak of IP1 (Fig. 6) shifts to lower angle, and the *d* spacing changes marginally from 4.36 to 4.4 Å.

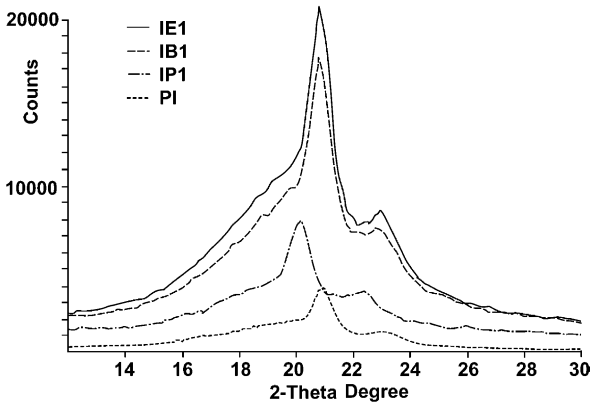

Fig. 6. Effect of various solvent on PE crystal morphology from WAXS (*Y* axis—a.u).

In general, the characteristic cluster has long-range order and appears in the low angle (<5°) region in X-ray scattering. The structure of the hybrid was also investigated using small angle X-ray scattering measurement (SAXS). Fig. 7 shows the SAXS profile of PI, IE1 and IB1. Intensity $I(q)$ is plotted against the scattering vector q (Fig. 8) [$q = (4\pi/\lambda)\sin(\theta/2)$, where λ is the wavelength of the X-ray (0.154 nm), θ is the scattering angle]. The ionomer has a sharp peak at around 0.69° (12.8 nm) due to scattering from the crystals in ionic domains. In the SAXS profile of the hybrid, the peak at 0.69° disappears, and a broad peak occurs at $2\theta = 0.3°$, which is assumed to be due to small clusters of silica. The radius of gyration (R_g) can be calculated from the following equation: $I(q) \propto e(-q^2R_g^2/3)$. Mauritz et al. [28] reported that the peak height of Nafion–silica hybrid decreases with increasing silica content. Embs et al. [29] also observed a broad peak at $q = 2$–$2.5\ \mathrm{nm}^{-1}$ for poly(*p*-phenylene vinylene)/silica hybrids due to the inter-domain spacing of silica. The power of $q(D)$ can be calculated from Fig. 8 according to $I(q) \propto kq^{-D}$ (k is constant), and is summarized in Table 4. Table 4 shows that silica morphology does not change with the amount of TEOS in the nonpolar solvent, but it does with the polar solvents. Silica in IB1 has a mixed morphology of a 3-D network and rough surface colloid, whereas silica is rougher and smooth surface colloid using the nonpolar solvent. This is because the interaction of ionic groups is lower in polar solvents. It allows more silica to reside in the cluster, with a facile growth of silica network. In the nonpolar solvent (IE1 and IE2), the cluster cannot dissolve and this restricts the insertion of silica. It is quite possible that part of the silica remains in the polymer matrix when the silica proportion is high. In our earlier communication [26], we reported that the cluster peak appears at $2\theta = 0.69°$ in the ionomer. In all the hybrids, the cluster peak shifts to low angle. The d spacing of the cluster thus increases after the sol–gel reaction. This result reveals that the cluster harbors silica after the sol–gel reaction, which is also evident from the DSC study.

TEM was used to evaluate the morphology of the hybrid.

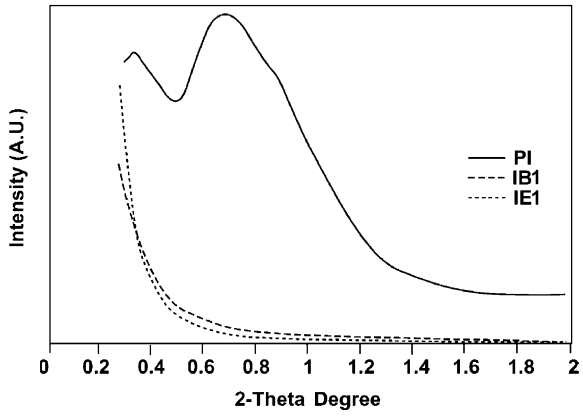

Fig. 7. Cluster structures of PI, IE1 and IB1 from SAXS measurement.

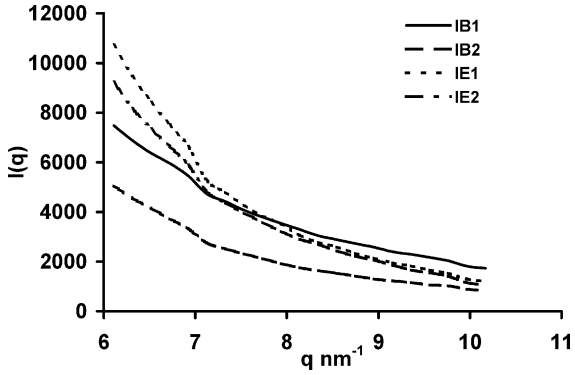

Fig. 8. $I(q)$ vs. q plots of IB1, IB2, IE1 and IE2.

TEM images of IB1 [23] and IE1 [24] have shown that very fine silica particles disperse homogeneously in the polymer matrix. Fig. 9(a) shows the TEM image of IP1. The white area shows the polymer matrix, and the dark area represents electron denser silica region. No phase separation is apparent. The silica particle size is in the molecular level. Thus the homogeneous dispersion of silica into the ionomer (which shows a featureless morphology in Fig. 9(b)) is achieved using various solvents.

3.5. Dynamic mechanical properties

DMA was used to obtain the dynamic mechanical properties of polymers. In our earlier work [23], we reported that the ionomer has four transitions. PE glass transition and the cluster transition occur at ~−130 and ~30 °C, respectively. Table 5 lists the storage modulus of the ionomer and the hybrids as a function of TEOS content at −140 °C and their cluster transition temperature. The glass transition of the polyethylene part occurs at about −130 °C, and does not change via the sol–gel reaction. This further confirms that silica formed from the sol–gel reaction does exist in the cluster part. The cluster transition temperature increases with decrease in the dielectric constant of the solvents. As shown in the SAXS results, the morphology of silica is different using different solvents. Individual silica particles are formed in less polar solvents, whereas silica networks appear in polar solvent. The adhesion between individual silica particles and ionic groups is better than a 3-D silica network. The storage modulus of the ionomer increases dramatically even at such low silica content. IE1 and IB1 have higher storage moduli than IP1 due to higher silica content and adhesion between silica particles and the

Table 4
D values and the morphology of silica for IB1, IB2, IE1 and IE2

Sample	*D* value	Silica morphology
IB1	2.85	3-D network and rough surface colloid
IB2	3.50	Rough and smooth surface colloid
IE1	4.26	Smooth surface colloid
IE2	4.15	Smooth surface colloid

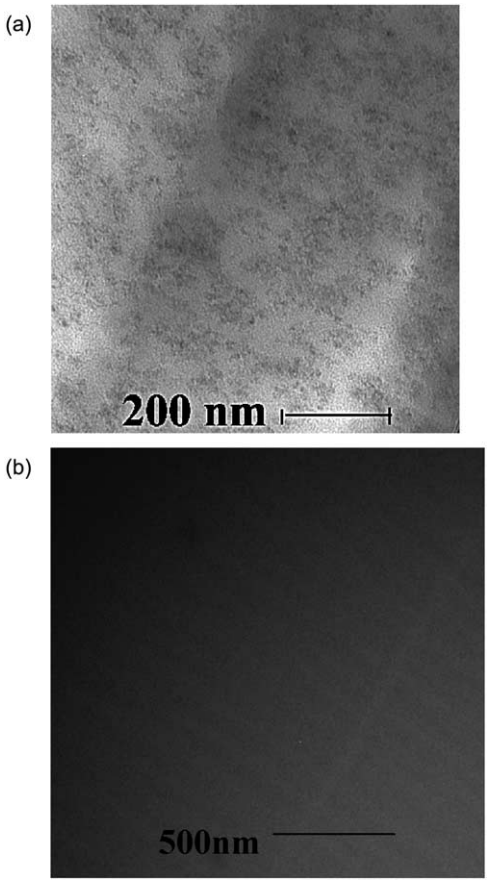

Fig. 9. (a), (b) Transmission electron micrograph of IP1 and PI.

ionic groups. The storage moduli of all the hybrids decrease with increasing temperature. The rubbery stage is obvious after 50 °C in each sample.

3.6. Effect of TEOS content

The other variable chosen to prepare PI–silica hybrids was TEOS proportion. The amount of TEOS generally determines the amount of silica formed in the matrix. Table 2 lists the effect of TEOS content on the nature of the sample and its optical clarity using the mixed solvent toluene and butanol. It is clearly seen that the sample is transparent at the ratio below and equal to 1, and the brittle nature of the sample appears when the ratio is above 1. The sample becomes more brittle with increasing TEOS. This is expected as the inorganic component disperses in the polymer matrix at a lower TEOS proportion, and the polymer disperses in the inorganic matrix at a higher TEOS content. Thus various amounts of TEOS in the ionomer can form different ionomer–silica hybrids with different properties.

Table 5
Storage modulus values at −140 °C of ionomer and the hybrids

Sample	Storage modulus MPa −140 °C	Cluster transition temp. °C
PI	4219	32.1
IE1	4995	40.7
IP1	4892	40.3
IB1	5006	37.2
–	–	–
IE2	4778	38.4
IP2	4334	40.2
IB2	4687	37.4

The structure and properties of the hybrids using 25% and 50% of TEOS with various solvents are also compared. As discussed above, solvents can affect the substructure of silica, but not the structure of the hybrids. When the amount of TEOS is changed without changing the solvent, the same phenomenon is observed. Fig. 10 shows the FTIR spectra of IP1 and IP2. The difference between these two curves is seen clearly only in two parts: the shoulder of the band at 1000–1200 cm^{-1}, and the peak related to –OH group at 3680 cm^{-1}. The intensity of the shoulder at 1000–1200 cm^{-1} reduces in IP1. This shows that the substructure of silica is affected by the TEOS content. Silica can have more cyclic substructure at high TEOS proportions. Siuzdak et al. [30] studied the structure of Surlyn–silica hybrid materials. According to them, more cyclic-structured silica is formed when the amount of TEOS is higher. Robertson and Mauritz [31] have studied the effect of silica proportion on the substructures of SP–silica (SP: the sulphonate side of the perfluoto (carboxylate/sulfonate) bilayer membrane) and CP–silica (CP: the sulfonate side of the perfluoro (carboxylate/sulfonate) bilayer membrane) hybrids. They observed that the linear substructure peak of CP–silica hybrid only appeared at higher silica proportion, but bigger with increasing silica content in SP–silica hybrids. The intensity of the band at 3680 cm^{-1} is also high with increasing amount of TEOS due to incomplete condensation reaction.

The thermal properties of the hybrids can be improved with increasing amount of TEOS due to the formation of more silica (Table 1: TGA results). However, the silica content in the hybrid is lower than the theoretically calculated value either due to the incomplete hydrolysis of

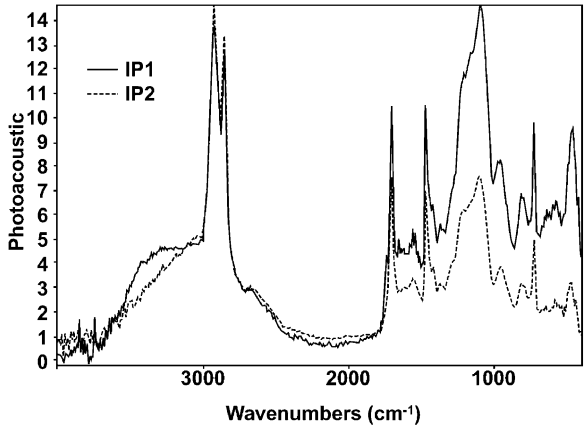

Fig. 10. FTIR spectra of IP1 and IP2.

the ethoxy group or the condensation of the silanol group. FTIR spectra (Fig. 1) show the existence of incomplete condensation and the effects of solvents on the substructures between Si–O–Si groups. The theoretical silica content of the sample can be calculated from the ratio of silica/TEOS. Table 6 lists the theoretical and experimental values of silica in the hybrids. The yield is higher at lower TEOS content. So the completion of reaction or the degree of the condensation is higher at lower TEOS percent. Thus, silica content in the hybrid is not affected by the solvents at low TEOS proportions.

The DSC and MDSC studies show that insertion of silica into the cluster takes place in all the hybrids with TEOS content. However, MDSC results (Table 3, Fig. 11) show that the total heat flow, reversing and nonreversing components are changed. More silica is formed at the high TEOS content, so the crystallinity of the hybrid at high TEOS content is lower. In addition, the total heat flow is reduced. The nonreversing component of all the hybrids with the low TEOS content is higher than that of the hybrids with the high TEOS proportion. However, the difference is significant between the hybrids using different solvent. For IB1 and IB2, not only the nonreversing component but also the contribution of nonreversing heat flow/total heat flow (NHF/HF) changes with reducing the amount of TEOS. For IP1 and IP2, and IE1 and IE2, the ratio of NHF/HF does not change with the TEOS proportion, although the nonreversing heat flow is higher at 25% TEOS.

The WAXS study shows that the *d* spacing of PE crystal does not change with TEOS contents (Fig. 12), but the peak area of melting reduces with increasing amount of TEOS due to restrictions imposed by silica on crystal growth.

The dynamic mechanical properties of the hybrids are affected by the presence of TEOS as seen from DMA results. Fig. 13 shows the temperature dependence of the dynamic viscoelastic property of the hybrids as a function of TEOS content. The onset of the decrease in the storage modulus is shifted to a higher temperature with increasing TEOS content (6 °C). The tan δ peak of IE1 is shifted slightly to a higher temperature than that of IE2 and the peak intensity also decreases. The improved mechanical properties of IE1 are due to higher proportion of silica. The cluster transition temperature also increases with increasing silica amount.

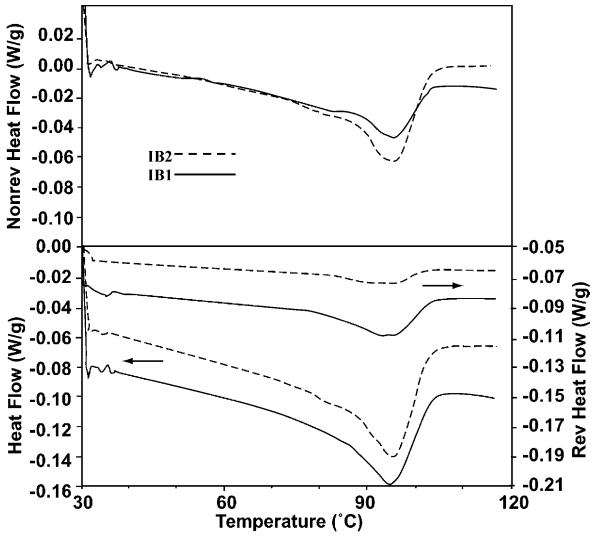

Fig. 11. MDSC thermograms of IB1 and IB2 at 2 °C/min.

3.7. Effect of H_2O/Si ratio

PI–silica hybrids were prepared at various ratios of H_2O/Si. The significant effect of the ratio on the sol–gel reaction was observed. The hybrid is transparent when the ratio is 1. When the ratio is equal or above 5, the sample becomes white. The higher the ratio, more silica particles can be seen. The sample loses transparency when the ratio varies from 1 to 10. This is due to the fact that a large amount of water causes phase separation during the sol–gel reaction. Tian et al. [32] observed phase separation at the ratio of H_2O/Si above 2 in preparing PCL–silica (PCL: poly ε-caprolactone) hybrids. Adding more water speeds up the hydrolysis reaction so that the hydrolysis of silicon alkoxide finishes before significant condensation occurred. Thus, the existence of a large amount of water delays the sol–gel process. This is also observed by Klein [33]. Tian et al. [32] also observed that a minimum in the gelation process occurs at H_2O/Si ratio 2. In the present case, a similar observation is made. The ratio of H_2O/Si affects the structure and morphology of PI–silica hybrids. At higher H_2O/Si ratio, the silica particles are in micrometer range due to partial aggregation; hence the properties of the composites are different from the nanocomposite hybrid.

4. Conclusion

PI–silica hybrid materials were synthesized via the sol–gel reaction using various H_2O/Si ratios, different TEOS

Table 6
Theoretical and experimental values of silica contents of the hybrids

Sample	IE1	IE2	IP1	IP2	IB1	IB2
Theoretical silica g	2.7	1.2	2.7	1.2	2.7	1.29
Experi. silica g	1.9	1.2	1.5	1.1	2.4	1.29
Degree of conversion %	71.5	99.1	55.9	89.8	88	100

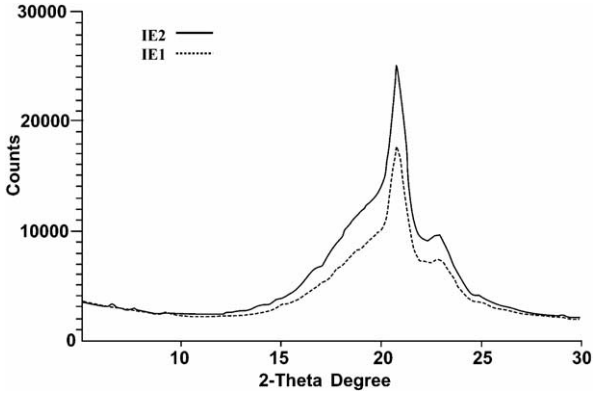

Fig. 12. Intensity vs. 2θ plot from WAXS of IE1 and IE2.

contents and solvents. The results show that the structure of the hybrids does not change with the change in these parameters, but the silica substructures and the thermal properties of the hybrids change.

The ratio of H_2O/Si is critical at 5, below which transparent hybrids can be obtained. Solvents do not affect the structure of the hybrids. However, the morphology of the silica network depends on the polarity of the solvents (SAXS). The degree of condensation reaction is solvent dependent as seen from ^{29}Si solid-state NMR. The thermal stability of the hybrid and the silica content are higher with polar solvents at high TEOS proportion, but are similar at the low TEOS content. The crystallinity of the hybrid decreases. Storage modulus increases with increased polarity of the solvents. The SAXS results show that silica resides in the cluster. The amount of TEOS affects the properties of the hybrids with TEOS content above 50 wt%, the hybrid becomes opaque and brittle. Below 50 wt% of TEOS, transparent samples can be obtained.

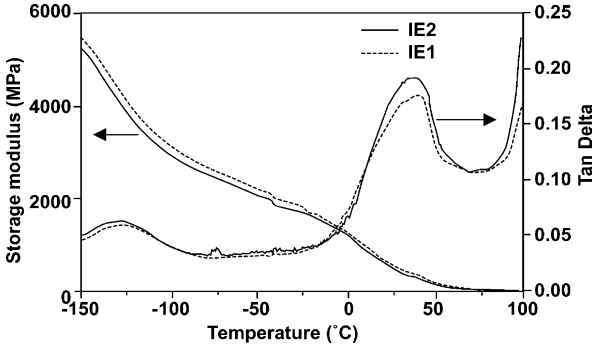

Fig. 13. Plot of storage moduli and tan δ vs. temperature of IE1 and IE2.

Acknowledgements

The authors would like to thank Mr Clint Gamlin of Ian Wark Research Institute for performing the SAXS work and Prof R. Weiss of University of Connecticut, USA for giving access to the SAXS instrument.

References

[1] (a) Mauritz KA, Storey RF, Reuschle DA, Beck Tan N. Polymer 2002;43(22):5949–58.
(b) Start PR, Mauritz KA. J Polym Sci Part B: Polym Phys 2003; 41(13):1563–71.
[2] Schiavon G, Kuchler JG, Corain B, Hiller W. Adv Mater 2001;13:310.
[3] Bandyopadhyay A, Bhowmick AK, de Sarkar M. J Appl Polym Sci 2004;93(6):2579–89.
[4] Wu KH, Yu CH, Chang YC, Horng DN. J Solid State Chem 2004; 177(11):4119–25.
[5] Jiang S, Yu D, Ji X, An L, Jiang B. Polymer 2000;41:2041.
[6] Keeling-Tucker T, Rakic M, Spong C, Brennan JD. Chem Mater 2000;12:3695.
[7] Deng Q, Wilkie CA, Moore RB, Mauritz KA. Polymer 1998;39(24): 5961–72.
[8] Musto P, Ragosta G, Scarinzi G, Mascia L. Polymer 2004;45(5): 1697–706.
[9] Juangvanich N, Mauritz KA. J Appl Polym Sci 1998;67:1799.
[10] Wen J, Wilkes GL. Chem Mater 1996;8:1667.
[11] Nell JL, Wilkes GL, Mohanty DK. J Appl Polym Sci 1990;40:1177.
[12] Greso AJ, Moore RB, Cable KM, Jarrett WL, Mauritz KA. Polymer 1997;38:1345.
[13] Wojcik AB, Klein LC. Appl Organomet Chem 1997;11:129.
[14] Yang JM, Chen HS, Hsu YG, Lin FH, Chang YH. Die Angewandte Makromolekulare Chemie 1997;251:61.
[15] Landry CJT, Coltrain BK, Brady BK. Polymer 1992;33:1486.
[16] Jonas J. Science of ceramic chemical processing. New York: Wiley; 1986. p. 52.
[17] Orcel G, Hench LL. J Non-Cryst Solids 1986;79:177.
[18] Zoppi RA, Yoshida IVP, Nunes SP. Polymer 1997;39:1309.
[19] Kim J-Y, Kim C-H, Yoo D-J, Suh K-D. J Polym Sci Part B: Polym Phys 2000;38:1903.
[20] Siuzdak DA, Mauritz KA. Polym Prep 1997;38(1):245.
[21] Siuzdak DA, Mauritz KA. J Polym Sci Part B: Polym Phys 1999;37:143.
[22] Stefanithis ID, Mauritz KA. Macromolecules 1990;23:2397.
[23] Gao Y, Choudhury NR, Dutta N, Matisons J, Reading M, Delmotte L. Chem Mater 2001;13:3644.
[24] Gao Y, Choudhury NR, Dutta N, Gamlin C, Matisons J, Delmotte L, et al. Second International Conference on Silica Science and Technology, Mulhouse, France 2001. p. 64.
[25] Wang S, Ahmad Z, Mark JE. Chem Mater 1994;6:943.
[26] Gao Y, Choudhury NR, Dutta N, Shanks R, Weiss B. J Therm Anal Calorim 2003;73:361.
[27] Cheng SZD, Chen J. J Polym Sci Part B: Polym Phys 1991;29:311.
[28] Mauritz KA, Stefanithis ID, Davis SV, Scheetz RW, Pope RK, Wilkes GL, et al. J Appl Polym Sci 1995;55:181.
[29] Embs FW, Thomas EL, Wang CJ, Prasad PN. Polymer 1993;34:4607.
[30] Siuzdak DA, Start PR, Mauritz KA. J Appl Polym Sci 2000;77:2832.
[31] Robertson MAF, Mauritz KA. J Polym Sci Part B: Polym Phys 1998; 36:595.
[32] Tian D, Blacher S, Jerome R. Polymer 1999;40:951.
[33] Klein LC. Ann Rev Mater Sci 1985;15:227.